DOE/NASA/3303-1
NASA CR-165385
ASRL TR 197-1

GENERAL REVIEW OF THE MOSTAS COMPUTER CODE FOR WIND TURBINES

John Dugundji and John H. Wendell
Aeroelastic and Structures Research Laboratory
Massachusetts Institute of Technology

June 1981

Prepared for
NATIONAL AERONAUTICS AND SPACE ADMINISTRATION
Lewis Research Center
Under Grant NSG-3303

for
U.S. DEPARTMENT OF ENERGY
Conservation and Renewable Energy
Division of Wind Energy Systems

NOTICE

DOE/NASA/3303-1
NASA CR-165385
ASRL TR 197-1

GENERAL REVIEW OF THE MOSTAS COMPUTER CODE FOR WIND TURBINES

John Dugundji and John H. Wendell
Aeroelastic and Structures Research Laboratory
Massachusetts Institute of Technology
Cambridge, Massachusetts 02139

June 1981

Prepared for
National Aeronautics and Space Administration
Lewis Research Center
Cleveland, Ohio 44135
Under Grant NSG-3303

for
U.S. DEPARTMENT OF ENERGY
Conservation and Renewable Energy
Division of Wind Energy Systems
Washington, D.C. 20545
Under Interagency Agreement DE-AI01-76ET20320

Acknowledgments

The authors would like to acknowledge helpful discussions with Prof. Rene H. Miller and Prof. Manuel Martinez-Sanchez during the course of this study. Also, they would like to acknowledge comments in the final phases by David C. Janetzke and Mark E. Dreier.

This research was carried out in the Aeroelastic and Structures Research Laboratory, M.I.T., and was supported by NASA Lewis Research Center under Grant No. NSG-3303, "Development of a Methodology for Horizontal Axis Wind Turbine Dynamic Analysis." The NASA Technical Officer for this work was David C. Janetzke, Wind Energy Project Office, NASA Lewis Research Center. The Principal Investigator was Prof. John Dugundji.

Abstract

The MOSTAS computer code for wind turbine analysis is reviewed, and the techniques and methods used in its analyses are described in some detail. Some impressions of its strengths and weakness, and some recommendations for its application, modification, and further development are made. Additionally, some basic techniques used in wind turbine stability and response analyses for systems with constant and periodic coefficients are reviewed in the Appendices.

Table of Contents

List of Principal Symbols

A	Equation coefficient matrix
B, B_g, B'_g	Damping coefficients
$b_{Ti}, b_{si}, b_{ci}, b_{Ai}$	Multiblade coordinates
b_T, b_A	Coordinates for 2-bladed rotors
c	Control input to blade, usually pitch change
C_x, C_β	Damping coefficients
C_L, C_D	Lift and drag coefficients
$E_g, E_c, E_w,$ $E_{\dot{w}}, E_{\ddot{w}}$	Eliminative equation coefficients
e	Eliminative variables
F, F_x, F_β	Force terms
f_o	Total rotor load at fixed shaft
f	Perturbation pod load applied to rotor
f_b	Fixed shaft blade loads
$\tilde{f}$	Perturbation blade loads
g	Wind velocity vector
I	Moment of inertia of blade
i	$\sqrt{-1}$
K, K_g, K'_g	Stiffness coefficients
K_I, k_I	Centrifugal stiffness terms
k_x, k_β	Stiffness coefficients
M, M_g, M'_g	Mass coefficients
m	Mass per unit length

N	Number of blades
P	Total load on blade from all sources
P	State equation coefficients
$\bar{p}$	External perturbation load on blade
p_o	Quiescent (static) load on blade
p_k	Eigenvalue
Q	Transition matrix
Q	State equation coefficients
q_i	Generalized coordinate
R	State equation coefficients
S	Basic blade load integral
S	Static moment of blade
s	Distance along blade
T	Period of oscillation
t	Time
V, V_g	External force coefficients
v	External forces
w	Independent variables
w_o	Quiescent (static) position of blade
x	Absolute rotor shaft displacements
Y	Matrix of eigenvectors
y	Rotor coordinates
Z	Matrix of eigenvectors

α	Control system coordinates
β	Modal coordinates of blade
γ	Teetering coordinate
γ, γ_R, γ_C	Torques
$\Delta_j(s)$	Mode shape of blade
δ	Tower base motion coordinates
ε	Small increment
η	Distance along blade
λ_k	Eigenvalue
ξ	Tower vibration mode coordinates
ϕ	Power train coordinates
ψ	Azimuth position = Ωt
ψ_k	Azimuth position of k^{th} blade $= \Omega t + (k-1)2\pi/N$
Ω	Rotation speed
ω	Natural frequency

1. Introduction

The purpose of this memorandum is to briefly review the MOSTAS Code models and solution methods; to outline some impressions of its strengths and weaknesses; and to suggest some modifications and tests of the models and analysis methods employed. Also, this memorandum reviews some basic techniques used in wind turbine stability and response analyses.

MOSTAS is a general computer analysis code for calculating the dynamic loads, and for investigating the aeroelastic and mechanical stability of horizontal axis wind turbines and helicopters.[1,2] It was originally developed for helicopters and later adapted to wind turbines. This review will be concerned with its application to wind turbines.

2. Typical Horizontal Axis Wind Turbine Analysis

To begin to evaluate MOSTAS, it is useful to imagine the steps one might take to perform a typical dynamic analysis of a horizontal axis wind turbine.

1. Derive equations of motion (partial differential equations or finite element models) for blades, tower, pod, and other system components. Also, formulate aerodynamic, inertial, and gravity loads.
2. Use equations of motion to calculate coupled normal modes ϕ_r, and natural frequencies, ω_r, for the blades.

These would preferably be rotating modes, although non-rotating modes could also be used. Calculate also normal modes and frequencies for the tower and other components.

3. Choose a sufficient number of modal coordinates q_i to adequately describe the motions of the system. Then derive modal equations for the q_i's from the equations of motion for the blades, tower, pod and other system components.
4. Couple entire system together.
5. Solve for the quiescent (static) blade response and corresponding static loads, bending moments, etc.
6. Solve for the dynamic blade response to the time-varying aerodynamic, inertial, and gravity loads. Calculate the dynamic loads to be added to the static loads. Investigate for any dynamic instabilities, both aeroelastic and mechanical in origin.

In attempting to carry out step 6, one often finds that the mass, stiffness, and damping terms for the blade equations contain periodic components in addition to the usual constant coefficients. For three or more bladed rotors, one can reduce most of these periodic components by introducing multiblade coordinates.[3] The equations can then be solved using standard, constant coefficient system response techniques. For a two or one bladed rotor, additional multiblade coordinates and harmonic balance methods need to be introduced to approximately eliminate the

periodic coefficients.[4] A crude method that has occasionally been used to deal with small periodic coefficients is to simply time-average the periodic variations over one blade revolution, thereby obtaining constant coefficient equations. However, unless the periodic coefficients are small, this may result in some errors and may miss some potential areas of instability. As a practical alternative to introducing multiblade coordinate and harmonic balance methods, one may directly integrate the periodic coefficient equations numerically and introduce Floquet techniques to examine the system for instability.[5,6]

The aerodynamic, inertial and gravity loadings on a wind turbine tend to occur periodically in multiples of the rotation frequency Ω. For constant coefficient equations, it is easiest to obtain the steady-state dynamic response to such loadings using frequency response techniques. These involve finding the harmonic response $q_j(t) = q_j e^{i\omega_m t}$ to each forcing frequency $\omega_m = m\Omega$, then summing up all the harmonic responses. See Appendix A. To investigate for instability, one recasts the dynamic equations in state-space form, determines the eigenvalues of the system, and notes if any eigenvalues are positive real, or have positive real parts. See Appendix A. For the direct numerical integration of the periodic coefficient equations, one picks a convenient integration scheme (Runge-Kutta, Newmark, Central Difference, etc.) and integrates from some initial condition. By proper choice of the initial condition, one can eliminate all

transients from the response and thereby show the desired steady-state dynamic response by integrating through only one blade revolution, instead of the very large number usually needed to reach steady-state for lightly damped systems. See Appendix B. To investigate these periodic coefficient equations for instability, one uses Floquet techniques, which implies finding the eigenvalues of the Transition Matrix. See Appendix B. The use of multiblade coordinate and harmonic balance techniques is described in Appendix C.

Having found the dynamic response by any of the methods outlined above, one may proceed to obtain the dynamic loads to be added to the static blade loads by summing all the additional applied aerodynamic, inertial, and gravity loads acting on the blade. This force summation method is preferable to the simpler mode deflection method since it represents the static loads more accurately, and it handles discontinuities better. Still, one should be careful to use a sufficient number of blade elastic modes to insure reasonable convergence in blade bending moments and shear.[7]

The typical analysis of horizontal axis wind turbines outlined here has several variations, depending on the authors. See for example, Spera,[8] Kottapalli and Friedmann,[5] Warmbrodt and Friedmann,[6] and Miller, et al.[9] A good general review and bibliography for dynamic analysis of such horizontal axis wind turbines has recently been given by Friedmann.[10] The specific steps and procedures used in MOSTAS will be described next.

3. Description of MOSTAS Code

3.1 General Layout

The MOSTAS Code is a very general computer formulation which attempts to include a wide variety of structural, inertial, aerodynamic, and generator system effects to obtain the dynamic loads on a wind turbine. The rotor may have one, two, or more blades which may be tapered, twisted, and preconed out of the plane of rotation. They may have cantilevered, hinged, or teetering attachments to the hub. The dynamics of the tower, pod, power train, and control system are considered in the analysis.

Basically, the MOSTAS Code can be divided into 3 sub-systems. See Fig. 1. First, there is the MOSTAB-HFW system which calculates the basic loads and bending moments f_b on an isolated single blade assuming a fixed shaft (i.e., no pod or tower motion), rotating at constant rotation speed Ω. Also, all the blades are combined to give total loads and moments f_o acting at the fixed shaft. Additionally, time varying, linear math models for the isolated single blade are generated in MOSTAB-HFW. Second, there is the ROLIM system, which is used to assemble a linearized model of the rotor from the isolated single blade models generated in MOSTAB-HFW. This linear rotor model includes multiblade coordinate transformations and is used in subsequent coupled analyses of the wind turbine. Finally, there is the WINDLASS system which couples the ROLIM produced linear rotor model with linear models of the pod, the tower, the control system, and the power train. This WINDLASS system produces small perturbation loads $\tilde{f}$, which are to be added on to

the basic MOSTAB-HFW fixed shaft loads f_b, to produce the final loads on the blades. The perturbation loads $\tilde{f}$ contain all the effects of the shaft motions and the rotor interactions with other components of the system. The input to this linear WINDLASS system are the fixed shaft, constant rotation speed rotor loads f_o, previously found by MOSTAB-HFW. Thus, the overall logic of the MOSTAS code is to concentrate mainly on the fixed shaft loads, which probably comprise the greater part of the blade load, then to add on the generally small corrections due to shaft motions and subsequent pod, tower, control system, and power train system interactions.

The above MOSTAS scheme here can be contrasted with some of the other analyses quoted earlier. Spera,[8] and Kottapalli and Friedmann[5] essentially analyze the fixed shaft system and hence are comparable to the MOSTAB-HFW portion of MOSTAS. See Fig. 1. Warmbrodt and Friedmann[6] include the effects of tower and pod motions, and hence would be similar to the WINDLASS portion of MOSTAS, but with the steady wind, wind shear, tower shadow, gravity, etc., input going directly into the rotor, rather than coming indirectly through the fixed shaft rotor loads f_o onto the pod. Miller et al.[9] consider the fixed shaft loads by harmonic decomposition into static loads, and using approximate dynamic magnification factors to obtain the dynamic loads. The effects of the tower motions are found by analyzing

simple tower-pod-rotor models.

The MOSTAS treatment of teetering rotors should also be mentioned. In order to calculate the fixed shaft loads f_b for such a teetering rotor, the teetering angle γ of the rotor must be known. Since this γ depends on the interactive motion of all the blades, a separate linearized analysis of the rotor blades is required. This is done as an additional small sub-loop in the MOSTAB-HFW system shown in Fig. 1. A linearized model of the rotor blades with teeter is constructed within MOSTAB-HFW; these are solved by a coupled linear analysis for the linear blade deflections and teetering angle; then this teetering angle is used to modify the total rotor load f_o feeding into the WINDLASS portion of the analysis, Fig. 1. This procedure seems a complex way to include the additional teetering degree of freedom γ, but it does adapt to the framework of the isolated blade model scheme of MOSTAB-HFW.

More specific details of the various MOSTAS component systems are described next.

3.2 MOSTAB-HFW System

The MOSTAB-HFW system deals with obtaining the dynamic loads and response of an isolated blade assuming a fixed shaft (i.e., no pod or tower motion), rotating at constant rotation speed Ω. It is essentially a modal analysis, and the blade motion is described by a superposition of blade natural vibration

modes added to a quiescent (static) blade position.

MOSTAB-HFW uses as input one to four blade natural modes and frequencies, the blade mass characteristics, the aerodynamic section characteristics, and the quiescent shape of the blade (the static shape before dynamic vibrations occur). It first proceeds to characterize the quiescent shape of a blade reference line (BRL) and a set of blade axes in terms of 3 translations and 3 Euler rotations from a set of rotor reference coordinates which rotate with the rotor. This is carried along numerically by a 6 x 1 column vector $w_o(s)$ for every point s on the BRL. Then it considers the blade vibration modes as small perturbations $\Delta_j(s)\ \beta_j(t)$ about the quiescent position $w_o(s)$. Each mode shape $\Delta_j(s)$ is again carried along as a 6 x 1 column vector, and by assuming the orthogonality properties of the given modes, the modal equations of motion can be expressed in the standard form,

$$\ddot{\beta}_i + \omega_i^2 \beta_i = M_i^{-1} \int_o^{\ell} \Delta_i^T \bar{p}\, ds \qquad (1)$$

where,

$$M_i = \int_o^{\ell} \Delta_i^T m\, \Delta_j\, ds$$

ω_i = Blade natural frequency

In the above procedure, all geometric nonlinearities are retained in characterizing the quiescent position of the blade $w_o(s)$, but small perturbation deflections are assumed for the subsequent vibrations. The given mode shape data $\Delta_j(s)$ and natural frequencies ω_j are usually taken as rotating blade modes (centrifugal force effects included). The external perturbation force $\bar{p}$

consists of all external perturbation loads except for the inertia loads and centrifugal stiffening loads (these have already been accounted for on the left-hand-side of Eq.(1)).

Rather than evaluating the generalized mass and generalized force integrals in Eq. (1) directly, the MOSTAB-HFW program prefers to mechanize all computations around repeated evaluations of the following integral,

$$S = \int_0^{\ell} \Delta_i^T(s)\ P(\beta, \dot{\beta}, \ddot{\beta}, s, t)\, ds \qquad (2)$$

where S is a desired integral and P is the total load on the blade from all sources (aerodynamic, inertial, centrifugal, gravity, etc.), and includes both linear and nonlinear effects. The external perturbation load $\bar{p}$ in Eq. (1) is related to the total load P by the relation,

$$\bar{p} = P - p_o + m\Delta_j \ddot{\beta}_j + k_I \Delta_j \beta_j \qquad (3)$$

where p_o is the quiescent (static) load on the blade, while $m\Delta_j\ddot{\beta}_j$ and $k_I\Delta_j\beta_j$ are the inertia and centrifugal stiffening loads that must be added in order to cancel out the corresponding loads $-m\Delta_j\ddot{\beta}_j$ and $-k_I\Delta_j\beta_j$ already present in the total load P.

The generalized mass term M_i in Eq.(1) is obtained from the general integral formula Eq.(2) by numerical differentiation.

First Eq. (2) is evaluated with all motions $\beta = \dot{\beta} = \ddot{\beta} = 0$ and all external perturbation loads $\bar{p} = 0$ in order to obtain the value, $S_o = \int \Delta_i^T p_o \, ds$. (See Eq. (3) rearranged to solve for P). A subsequent evaluation with $\ddot{\beta}_j = \epsilon$ (where ϵ is a small positive value) and all other $\ddot{\beta} = \dot{\beta} = \beta = 0$ will yield $S_\epsilon = S_o - \epsilon \int_o^\ell \Delta_i^T m \Delta_j \, ds$ Then,

$$M_{ij} = - \frac{S_\epsilon - S_o}{\epsilon} \qquad (4)$$

A similar numerical differentiation procedure with $\beta_j = \epsilon$ and all other $\ddot{\beta} = \dot{\beta} = \beta = 0$ will yield the linear stiffening terms $K_{I\,ij}$. Finally, the generalized force in the basic Eq. (1) is evaluated by placing the $\bar{p}$ given by Eq. (3) into the integral formula Eq. (2) to obtain the right-hand-side of Eq. (1) as,

$$M^{-1} \int_o^\ell \Delta_i^T \bar{p} \, ds = M^{-1} [S - S_o] + \ddot{\beta} + M^{-1} K_I \beta \qquad (5)$$

In the above, all matrix expressions M, S, S_o, K_I have been obtained by using repeated evaluations of the general integral formula Eq. (2). The $\ddot{\beta}$ term appearing in Eq. (5) is present in order to cancel the corresponding inertia forces present in the total load term S.

The aerodynamic loads in the total load P are calculated assuming quasi-steady strip theory, and static stall effects are included by using curve-fit functions, C_L and C_D versus angle

of attack. Geometric nonlinearities are retained since angles of attack are found numerically. The inflow of air may vary over the disk in accordance with simple momentum theory which treats independent annular volumes of air. Also, inflow corrections can be made for wind shear, tower shadow, and rotor tip losses.

The equations of motion, Eq.(1) with the right-hand-side expressed by Eq.(5) are of the general form,

$$\ddot{\beta}_i + \omega^2 \beta_i = g_i\left(\beta_j, \dot{\beta}_j, \ddot{\beta}_j, t\right) \qquad (6)$$

These equations are integrated numerically around one rotor revolution, from $\psi = \Omega t = 0$ to $\psi = 2\pi$, for a given set of initial conditions on β and $\dot{\beta}$. The correct initial conditions that will result in steady-state, periodic solutions, are found using the procedure described in Appendix B. The numerical integration method used in MOSTAB-HFW consists of assuming g_i to be constant over some small azimuth interval $\Delta\psi = \Omega \Delta t$. The equations are then uncoupled, and a conventional solution over that interval is given as,

$$\beta_{k+1} = \left(\beta_k - \frac{g_k}{\omega^2}\right) \cos \omega \Delta t + \frac{\dot{\beta}_k}{\omega} \sin \omega \Delta t + \frac{g_k}{\omega^2} \qquad (7)$$

$$\dot{\beta}_{k+1} = -\left(\beta_k - \frac{g_k}{\omega^2}\right) \omega \sin \omega \Delta t + \dot{\beta}_k \cos \omega \Delta t$$

$$\ddot{\beta}_{k+1} = -\omega^2 \left(\beta_{k+1} - \frac{g_{k+1}}{\omega^2}\right)$$

Care must be taken that the time interval $\Delta t = \Delta\psi/\Omega$ is sufficiently short for the highest natural frequency ω_n involved, otherwise numerical instability results ($\Delta t < 2\pi/5\omega_n$). Some schemes for suppressing the numerical instability are discussed, so that excessively small azimuth intervals (and hence excessive computer time) need not always be used.

Having obtained the required time histories $\beta, \dot{\beta}, \ddot{\beta}$ over one rotor revolution, the desired shears and bending moments f_b for an isolated blade are found from the relation,

$$f_b = \int_s^\ell R(s,\eta)\ P(\beta, \dot{\beta}, \ddot{\beta}, \eta, t)\, d\eta \qquad (7)$$

where f_b is a 6 x 1 column vector representing the 3 total shears and 3 total bending moments at any point s on the blade, and P is the total load on the blade from all sources (aerodynamic, inertial, centrifugal, gravity, etc.). The above relation Eq.(7) is essentially a "force summation" method instead of a "mode displacement" method for the loads, and it is evaluated using the familiar set-up for the general integral formula Eq.(2), only now $\Delta_i^T(s)$ is replaced by some other function $R(s,\eta)$, and the lower limit o is replaced by the more general value s.

The isolated blade load time histories f_b computed above are additionally fourier-analyzed to obtain the amplitudes and phase angles of the lowest few harmonics involved. The loads

from each individual blade can then be combined together to form the fixed shaft load input f_o to the WINDLASS system as described in Section 3.1.

Additionally, time varying, linear math models for the isolated single blade are generated in MOSTAB-HFW. This is accomplished apparently by combining the modal equations of motion Eq. (1), with numerical differentiation of the general integral formula Eq. (2), to obtain $\ddot{\beta}$, $\dot{\beta}$, and β coefficients similar to the manner described in Section 3.2 for obtaining the generalized mass term M_{ij}. This is done at many azimuthal locations of the blade. Because of the numerical differentiation, all nonlinear effects are included in the derivative calculations.

Finally, it should be mentioned that for the case of a teetering rotor, the calculation of the fixed shaft loads f_b is considerably more complicated since the interactive motion of all the blades must be considered. This involves doing, (in the MOSTAB-HFW system), a coupled linear analysis of the teetering degree of freedom γ with the given modes of all the blades, as was described briefly at the end of the previous Section 3.1.

3.3 ROLIM System

From details inferred in Refs. 1 and 2, the ROLIM system basically assembles a linear (perturbation) math model of the entire rotor about the trim operating condition, from the linear math models of the isolated single blades generated in the MOSTAB-HFW analysis.

The isolated single blade model is expanded to represent the full N-bladed rotor by assembling each set of modal coordinates in a stacked fashion,

$$\left\{ \begin{array}{c} \beta_i^{(1)} \\ \vdots \\ \beta_i^{(2)} \\ \vdots \\ \beta_i^{(3)} \\ \vdots \end{array} \right\}$$

where $\beta_i^{(k)}$ are the M modal coordinates of the k^{th} blade, and the coordinates of each blade are assumed to be shifted in azimuthal phase an amount $\Delta\psi = 2\pi/N$ from its neighbor. In addition to the above blade coordinates $\beta_i^{(k)}$, one has 6 additional rotor shaft coordinates x_i, representing possible displacements of the rotor hub in three directions, and possible rotations of the rotor hub about three axes due to motion of the tower and pod. The equations of motion are expanded to include these additional hub translation and rotation effects. Because the rotor hub motions are described in a fixed reference frame while the blade motions are described relative to a rotating reference frame, the resulting equations of motion will generally have mass, damping, and stiffness coefficients which are now periodic functions of azimuth position of the k^{th} blade, ψ_k.

For rotors with 3 or more blades, it is known that the periodic coefficients in the above equations can be largely cut down and reduced to constant coefficients by introducing multiblade coordinates b_{Ti}, b_{1si}, b_{1ci}, b_{2si}, ... such that,

$$\beta_i^{(k)} = b_{Ti} + b_{1si}\sin\psi_k + b_{1ci}\cos\psi_k + b_{2si}\sin 2\psi_k + b_{2ci}\cos 2\psi_k + \cdots + b_{Ai}(-1)^{k-1} \tag{8}$$

where $\psi_k = \Omega t + (k-1)\,2\pi/N$ represents the azimuthal position of the k^{th} blade and the number of coordinates taken equals the number of blades, N. See Appendix C. The ROLIM system introduces such multiblade coordinates and resulting equations of the entire rotor are recast in the matrix form,

$$M\ddot{y} + P\dot{y} + Qy = R(f, c, \Omega, g) \tag{9}$$

where M, P, Q, are constant coefficient square matrices, and y is a column matrix of the unknown coordinates,

$$y = \begin{Bmatrix} x_i \\ b_{Ti} \\ b_{1si} \\ b_{1ci} \\ \vdots \end{Bmatrix} \tag{10}$$

The first 6 coordinates x_i in y above represent the rotor shaft motions while the remaining b_i's, etc. are the multiblade

coordinates. The right-hand-side R represents the effects of forces and moments acting on the rotor and is considered a function of,

f - forces and moments from nacelle pod to rotor hub.

c - control inputs to the blade angles.

Ω - speed of rotation.

$\dot{g}$ - wind velocity vector.

The above linear model of the rotor system Eq. (9), is then used in the subsequent rotor-tower interaction system WINDLASS described in the next section.

The second order Eqs. (9) can also be rewritten in the state-space form as twice as many first order equations,

$$P\dot{y} - Qy = R(f, c, \Omega, \dot{g}) \qquad (11)$$

where the matrices P, Q, R, and y now have different definitions and dimensions. See Appendix A. ROLIM assembles some of its analyses in the form of Eqs. (11) as well as Eqs. (9).

Some comments should be made about the use of multiblade coordinates when the number of blades N < 3. For 2-bladed rotors, N = 2, the multiblade coordinates Eq. (8) will not eliminate the periodic terms. Rather, it will introduce the two coordinates $b_{Ti}(t)$ and $b_{Ai}(t)$ which together with x_i, can then be expanded in a harmonic series,

$$
\begin{aligned}
x_i &= x_{oi} + x_{1si}\sin\Omega t + x_{1ci}\cos\Omega t + x_{2si}\sin 2\Omega t + \cdots \\
b_{Ti} &= b_{Toi} + b_{T1si}\sin\Omega t + b_{T1ci}\cos\Omega t + \cdots \\
b_{Ai} &= b_{Aoi} + b_{A1si}\sin\Omega t + b_{T1ci}\cos\Omega t + \cdots
\end{aligned}
\tag{12}
$$

where x_{oi}, x_{1si}, b_{Toi}, b_{T1Si}, ... are all functions of time. The harmonic balance method can then be applied to obtain approximate solutions as discussed in Appendix C. The resulting response will then consist of a fundamental frequency plus various harmonics of frequency $m\Omega$, where m is an integer.

The ROLIM system introduces a special form for the multi-blade coordinates for a two-bladed rotor, namely,

$$
\begin{aligned}
\beta_i^{(k)} &= b_{oi} + b_{si}\sin\psi_k + b_{ci}\cos\psi_k \\
\dot{\beta}_i^{(k)} &= \dot{b}_{oi} + \Omega b_{si}\cos\psi_k - \Omega b_{ci}\sin\psi_k
\end{aligned}
\tag{13}
$$

where for N = 2, one has $\psi_k = \Omega t + (k-1)\pi$. In matrix form this appears as,

$$
\begin{Bmatrix} \beta^{(1)} \\ \dot{\beta}^{(1)} \\ \beta^{(2)} \\ \dot{\beta}^{(2)} \end{Bmatrix} = \begin{bmatrix} 1 & 0 & \sin\psi_1 & \cos\psi_1 \\ 0 & 1 & \Omega\cos\psi_1 & -\Omega\sin\psi_1 \\ 1 & 0 & -\sin\psi_1 & -\cos\psi_1 \\ 0 & 1 & -\Omega\cos\psi_1 & \Omega\sin\psi_1 \end{bmatrix} \begin{Bmatrix} b_o \\ \dot{b}_o \\ b_s \\ b_c \end{Bmatrix} \tag{14}
$$

This is placed into Eqs.(6) written in state-space form (i.e., as first order equations), and after adding the hub motion coordinates x_i and multiplying by the transpose of the above transformation, one obtains equations of the form of Eq.(11) where y now represents the variables x_i, $\dot{x}_i$, b_o, $\dot{b}_o$, b_s, b_c.

The transformation Eq. (14) is a mathematically valid one, and it appears efficient since it represents the 4 unknowns $\beta^{(1)}$, $\dot{\beta}^{(1)}$, $\beta^{(2)}$, $\dot{\beta}^{(2)}$ in terms of 4 new unknowns b_o, $\dot{b}_o$, b_s, b_c, and also, it tends to change the sin ψ_1 variations into sin $2\psi_1$ variations. However, Kaza, Janetzke and Sullivan[2] pointed out by application to a simple example, that if one subsequently time-averages out the resulting sin $2\psi_1$ and cos $2\psi_1$ variations to zero, it gives poor results for the frequencies and instability regions.

A somewhat better transformation to use for these 2-bladed rotors is the following,

$$\beta_i^{(k)} = b_{oi} + b_{si} \sin\psi_k + b_{ci} \cos\psi_k \tag{15}$$

or in matrix form, this appears as,

$$\begin{Bmatrix} \beta^{(1)} \\ \dot{\beta}^{(1)} \\ \beta^{(2)} \\ \dot{\beta}^{(2)} \end{Bmatrix} = \begin{bmatrix} 1 & 0 & \sin\psi_1 & 0 & \cos\psi_1 & 0 \\ 0 & 1 & \Omega\cos\psi_1 & \sin\psi_1 & -\Omega\sin\psi_1 & \cos\psi_1 \\ 1 & 0 & -\sin\psi_1 & 0 & -\cos\psi_1 & 0 \\ 0 & 1 & -\Omega\cos\psi_1 & -\sin\psi_1 & \Omega\sin\psi_1 & -\cos\psi_1 \end{bmatrix} \begin{Bmatrix} b_o \\ \dot{b}_o \\ b_s \\ \dot{b}_s \\ b_c \\ \dot{b}_c \end{Bmatrix} \tag{16}$$

This transformation represents the 4 unknowns $\beta^{(1)}$, $\dot{\beta}^{(1)}$, $\beta^{(2)}$, $\dot{\beta}^{(2)}$ in terms of 6 new unknowns b_o, $\dot{b}_o$, b_s, $\dot{b}_s$, b_c, $\dot{b}_c$, and upon substitution into the equations of motion and multiplying by its transpose, it will lead to 6 blade equations instead of the 4 obtained by the previous transformation, Eq. (14). Although this does not appear as efficient as the previous transformation,

it allows more flexibility among the coordinates and gives much better results if one subsequently time-averages the resulting sin $2\psi_1$ and cos $2\psi_1$ variations to zero. It gives reasonable frequencies and it will preserve the instability regions (slightly shifted). See Refs. 4 and 14.

It would appear then, that ROLIM would do better using the transformation Eq. (16) with time-averaging to obtain constant coefficient equations rather than using the special form, Eq. (14) with time-averaging. Otherwise, if the special transformation Eq. (14) is used, one should solve the resulting equations and check their stability using Floquet techniques, as discussed in Appendix B, or by some other scheme which includes the periodic coefficients in the equations. This was also suggested in Ref. 2.

3.4 WINDLASS System

The WINDLASS system couples together linear models of the rotor, the nacelle pod, the tower, the control system, and the power train, to give the dynamic response of the overall system. The main input to the WINDLASS system is the fixed shaft, constant rotation speed loads f_o, previously found by MOSTAB-HFW and applied to the nacelle pod. This sets up small perturbation responses everywhere in the overall coupled dynamic system. The total loads on the blades are then taken as the sum of the fixed shaft loads f_b and the additional perturbation loads $\tilde{f}$ due to the nacelle pod motions. Figure 2, taken from Ref. 1, shows a block diagram of the overall WINDLASS system, its five subcomponents, its variables, and the general form of its equations. A brief description of the various subcomponents follows.

The linear rotor model is developed by the ROLIM system from the MOSTAB-HFW analysis and was described in the previous section. The governing equations are given by Eqs. (9) or (11) and the variables y are given by Eq.(10). The first six of the variables y represent the six absolute rotor shaft motions x, while the remaining variables represent the multiblade coordinates b_{Ti}, b_{si}, . . . for the rotor blades. The various inputs to the equations, f, c, Ω, g are also described in the previous section on ROLIM.

The nacelle pod acts as an interfacing device that connects the rotor, tower, control system, and power train systems together. The pod itself is modeled as a massless elastic spring superimposed with an infinitely rigid mass, so that the pod model has no relative structural vibration modes, but it does contribute its mass properties to the overall system dynamics. The yaw drive spring stiffness plays an important role in the nacelle pod representation. The form of the governing equations for the pod can be seen in Fig. 2. The fixed shaft rotor loads f_o are the primary forcing function on the pod, while f is the perturbation load from the pod to the rotor. The f_T are loads from the pod to the tower top, x_T is the absolute position of the tower top, f_M are the loads applied to the pod rigid body mass, x_M is the absolute position of the pod rigid mass, and γ_R is the torque from the rotor to the power train. The remaining subscripted f, x, and γ variables represent various intermediate loads, positions, and torques.

The tower model is represented by its natural modes of vibration ξ. These are found from a separate finite element analysis of the tower, and are usually performed using a mass at the top to approximate the mass properties of the nacelle-rotor unit. The resulting modes and frequencies then give a more accurate description of what the tower is doing during its system coupled motion. However, the effect of this mass has

to be subtracted out from the model of the isolated tower used in the WINDLASS system. Also, the effect of the elastic tower mounted on a flexible base is also included so that one might additionally consider a movable soil. Six additional degrees of freedom δ, representing rigid body motions of the base, are included in the tower model, and appropriate equations are developed. The form of the governing equations for the tower are shown in Fig. 2, one set representing the predominantly elastic tower vibration modes ξ, the other representing the predominantly base vibration modes δ. The f_T are the loads from the nacelle pod to the tower top, the x_T is the absolute position of the tower top, and the f_{ET} are external applied loads to the tower such as due to drag or cables. It would seem the tower model could probably be simplified by including flexible soil effects as a simple reduction in the tower natural frequency, instead of introducing six additional degrees of freedom.

The control system model represents the power machinery, power machinery controls, utility network dynamics, rotor speed controller, and other servo-systems present to regulate the speed of the wind turbine. A simple such model is shown in Fig. 2. Here h represents the command inputs to the system; i.e., the desired speed or the speed governor, the α represents the control system degrees of freedom, and ϕ and $\dot{\phi}$ represent the angular position and velocity of some gear of the rotor shaft.

The controller generates a rotor control input c from the control system degrees of freedom α, which is then fed into the rotor to control its behavior. The control input c usually represents a rotor collective pitch change θ_o. The associated torques on the power train γ_c and nacelle pod γ_{cp} are also generated from the control system degrees of freedom α.

The power train model represents the assembly of gears, shafts, and generator that make up rotating parts of the wind turbine. The WINDLASS system makes up the power train by connecting a series of basic modules, each of which consists of a large main gear, a small pinion gear and an interconnecting elastic shaft. The smaller pinion gear is considered massless, and two damping coefficients are considered, one for the shaft and one for the bearings. Additionally, the torques transmitted through the system and to the supporting bearings are also considered. The form of the governing equations for the power train are shown in Fig. 2. Here ϕ represents the power train degrees of freedom which relate to the angular position of each gear, while γ_E represents the sum of the torques acting on the power train coming from the rotor γ_R, from the control system γ_c, and from externally applied torques γ_{EP}. The rotor speed Ω is related to ϕ, and the γ_B represents the base torque loads on the pod.

The equations of motion for the five subcomponents of the WINDLASS system and their interrelationship is shown in Fig.2. It remains to assemble all the equations together into a convenient form to solve them simultaneously. Since the wind turbine system was developed, for the sake of generality, as a series of independent blocks linked together, the equations as presented include displacements and interface force terms as variables. To solve such a large set of equations is unwieldy since not only are there many variables, but also the deflection and force operators may contain terms of widely varying magnitude which may cause numerical problems. To reduce the size of these equations, the WINDLASS procedure separates the variables into two groups - an "independent" group, usually comprising the displacements, and an "eliminative" group, usually comprising the interface forces. The equations are then also separated into independent and eliminative equations so that they can be written as,

$$\begin{aligned} M_g \ddot{w} + B_g \dot{w} + K_g w &= E_g e + V_g v \\ E_e e &= E_w w + E_{\dot{w}} \dot{w} + E_{\ddot{w}} \ddot{w} + E_v v \end{aligned} \tag{17}$$

where w represents the independent variables, e represents the eliminative variables, and v represents the externally applied

loads. The e variables can then be eliminated by solving the second equation for e and placing into the first equation to yield a smaller set of equations,

$$M_g' \ddot{w} + B_g' \dot{w} + K_g' w = V_g' v \qquad (18)$$

where,

$$M_g' = M_g - E_g E_e^{-1} E_{\ddot{w}}$$

$$B_g' = B_g - E_g E_e^{-1} E_{\dot{w}}$$

$$\vdots \qquad \text{, etc.}$$

After solving the smaller set of Eqs. (18) for w, the eliminative variables e are obtained from the second equation Eq. (17) by multiplying by E_e^{-1}. It should be noted that in the above reduction procedure, the eliminative variables e never appear as time derivatives in the equations of motion. Hence the order of the differential equation system in Eqs. (17) is the same as that in Eq. (18) even though Eq. (18) has fewer variables. Thus no essential dynamics has been lost. Also, it should be noted that this reduction procedure requires the matrix E_e to be nonsingular. Often, because of the choice of variables and the existence of constraints, E_e is singular. In such cases, a special processing technique is used to get around this by first using linear algebra techniques to express the

matrix E_e in the form,

$$E_e = C^{-1} D B \tag{19}$$

where C and B are nonsingular matrices and D is the identity matrix except for zeros in the first n rows corresponding to the order of the singularity in E_e. This form isolates the singularity and allows one to rewrite Eqs.(17) in the same form as before, only now w has n additional variables, the M_g, B_g, K_g, V_g, E_w, $E_{\dot{w}}$, $E_{\ddot{w}}$, E_v matrices are defined somewhat differently, and E_e becomes the unit matrix. The reduction to the smaller set of Eqs.(18) then follows.

The WINDLASS system can solve the assembled linear equations of motion Eqs. (18) by either using frequency response methods or by using direct numerical time integration methods. Originally, only the frequency response method was available, but later, the time integration method was added.

In the frequency response method, the forcing functions v which generally occur periodically over a cycle of turbine revolution, are broken down into their harmonic components. The harmonic responses w are then found and added together to give the total response, as shown in Appendix A. The WINDLASS subprogram to obtain the frequency response, Eqs. (A-8) and (A-9) is designated DYNAM2, while the subprogram to recover the time history Eq.(A-10) is designated RECOV2. The total loads acting

on the blades f_{TOT} are then found by summing the original fixed loads f_b and the here calculated perturbation loads $\tilde{f}$. Also if desired, the blade response relative to the rotating system $\beta^{(k)}$ can be obtained from the multiblade coordinate transformation Eq. (8). It should be noted that this frequency response method as discussed in Appendix A requires that the Eqs. (18) have constant coefficients. If the equations have periodic coefficients, the periodic parts must be time-averaged over one cycle, and only the constant portions used. This may lead to some errors for 2-bladed rotors, particularly if the specialized 2-bladed multiblade coordinate transformation, Eq. (14) is used. See Ref. 2. The overall MOSTAS system using DYNAM2 and RECOV2 is labeled as MOSTAS-A in Ref. 2.

The time integration method of solving Eqs. (18) is convenient for arbitrary time varying loads applied to the structure (such as wind gusts), and it allows any periodic coefficients in Eqs. (18) to be accounted for. The equations of motion Eqs. (18) could be numerically integrated by any of the standard numerical techniques such as Runge-Kutta, Newmark, Central Differences, Houbolt, etc., to get the response. However, because of the very general nature of the assembly methods, there may be constraints among the various chosen coordinates w such that they are not truly independent, and hence the mass matrix M may be singular. To get around this singularity, WINDLASS makes use of eigenvalue analysis to arrive at the

following numerical integration method. First, it rewrites Eqs. (18) in first order form,

$$P\dot{y} - Qy = Rv \tag{20}$$

where the matrices P, Q, R, v, y, are defined by comparing with Eqs. (A-2) and (A-1) of Appendix A. Then, it separates out the time-averaged constant parts P_o, Q_o from the periodic parts $\bar{P}$, $\bar{Q}$, of the P, Q matrices and rewrites Eqs. (20) as

$$P_o\dot{y} - Q_o y = Rv - \bar{P}\dot{y} + \bar{Q}y \tag{21}$$

where the entire right hand side will be treated as a constant forcing function over small time intervals Δt in the subsequent numerical integration process. Next, using eigenvalue analysis, the program finds the eigenvalues λ_i and eigenvectors y_i, z_i of the homogeneous system $P_o\dot{y} - Q_o y = 0$ and of its transpose $P_o^T\dot{z} - Q_o^T z = 0$. Since the matrices P_o and Q_o may in general be singular, the eigenvalues λ_i and eigenvectors y_i and z_i are found using special linear algebra methods described in Ref. 11 which first take out the singularities in P_o and Q_o. The resulting eigenvectors y_i are arranged, column by column, in an array Y called the modal matrix. Similarly, the z_i are arranged into another modal matrix Z. Then introducing new coordinates q such that $y = Yq$ and multiplying Eq. (21) by Z^T, the program

obtains the equations of motion as

$$G\dot{q} - Hq = c(q, \dot{q}, t) \tag{22}$$

where,

$$G = Z^T P_o Y$$

$$H = Z^T Q_o Y$$

$$c = Z^T R v - Z^T \bar{P} Y \dot{q} + Z^T \bar{Q} Y q$$

Reference 11 shows that G and H are diagonal matrices due to the orthogonality properties of the modal matrices Y and Z, and they are nonsingular. These matrix equations can then be rewritten in the equivalent form,

$$\dot{q} - \Lambda q = G^{-1} c \tag{23}$$

where $\Lambda = G^{-1}H$ is a diagonal matrix of the eigenvalues λ_i free of zeros. Since Λ is diagonal and c can be assumed constant over a small time interval Δt, Eqs.(23) are seen to be uncoupled, and each equation can be solved independently to give

$$q_i(t+\Delta t) = \left[q_i(t) + \frac{c_i}{G_i \lambda_i}\right] e^{\lambda_i \Delta t} - \frac{c_i}{G_i \lambda_i} \tag{24}$$

where $\lambda_i = H_i/G_i$ and is generally complex. This numerical integration scheme is the first order complex counterpart of that used in MOSTAB-HFW involving second order real equations, Eqs. (6) and (7).

Finally, after solving for q, the physical coordinates are obtained through the transformation y = Yq, and the time

histories of the blade loads f_{TOT} are obtained as before by summing the original fixed shaft loads f_b and the here calculated perturbation loads $\tilde{f}$. In the above procedure for integrating Eqs.(18), it should be mentioned that for practical expediency, the number of degrees of freedom is substantially reduced prior to the solution. This is done by discarding the very high frequency modes in Eqs.(18). Otherwise, time integrations of these equations would be extremely difficult.

The WINDLASS subprogram that performs the numerical time integration method here is designated WINDGUST, and can be used to obtain the response to any forcing function v in Eqs. (20) subject to any initial conditions. For forcing functions which occur periodically over one cycle of turbine revolution, the resulting steady-state response can be found by integrating over only one cycle rather than many cycles provided the proper initial conditions are found. WINDGUST uses the scheme described in Appendix B for this purpose. The overall MOSTAS system using the time integration WINDGUST subprogram is labeled as MOSTAS-B.

Summarizing the two methods of solving the linear equations of motion, MOSTAS-A uses frequency response methods (DYNAM2 and RECOV2) to solve Eqs.(18) with time-averaged coefficients, while MOSTAS-B uses time integration methods (WINDGUST) to solve Eqs. (21) with the periodic coefficients $\overline{P}$ and $\overline{Q}$. From an investigation by Kaza, Janetzke, and Sullivan[2], MOSTAS-B seems to do better for the forced response than MOSTAS-A when applied to

2-bladed rotors, since it takes into account the periodic coefficients $\overline{P}$ and $\overline{Q}$ of Eqs.(21). On the other hand, MOSTAS-A seems a simple and efficient method of getting the harmonic response when periodic coefficients are small, as in 3-bladed turbines.

For investigating the stability of the rotor systems given by the assembled linear Eqs. (18), the WINDLASS system sets the forcing functions v = 0, then time-averages the coefficients to constant values, then obtains the eigenvalues p_k of the system and notes if any are positive or have positive real parts. See Appendix A. Because the mass matrix M is often singular, the methods previously described for the WINDGUST analysis, Eqs. (20) to (23) are used to get around this singularity. In fact, the eigenvalues $\lambda_i = G_i/H_i$ found from Eqs. (22) are exactly the desired eigenvalues p_k to be examined for stability. Hence, the previous WINDGUST response analysis automatically includes the stability investigation of the time-averaged constant coefficient system.

To examine the stability of Eqs. (18) when periodic coefficients are present, Floquet methods should be introduced as described in Appendix B. It does not appear in Ref. 1 that this has been incorporated into the WINDLASS analysis, but in any event, its inclusion is simple since it involves merely finding the eigenvalues λ_k of the "transition matrix" Q defined in Eq. (B-5). This

matrix Q has already been formed by WINDGUST to obtain the proper initial conditions for steady-state response. Appendix B. If any of its eigenvalues λ_k has a magnitude equal to or greater than unity, the system is unstable. Alternatively, a root perturbation method is currently being considered for investigating the stability of the periodic coefficient systems.

As mentioned earlier, the use of the time-averaged constant coefficient method should be used with caution when dealing with 2-bladed rotors. See Kaza, Janetzke, and Sullivan[2], and the discussion earlier in Section 3.3. This is apparently due to the nature of the 2-bladed transformation, Eq.(14) used in ROLIM.

4. Strengths and Weaknesses of MOSTAS

The MOSTAS code for wind turbine analysis seems to be a very general code incorporating some interesting features, which has been built up over the years to handle a variety of helicopter and wind turbine problems. Many additions have been made to the original base to make the routine more general, and many sophisticated data processing technqiues have been added accordingly to handle these. As a result, one begins to lose the feel of what is going on in the structure, and one wonders if numerical accuracy is beginning to obscure even simple results.

The following are some specific comments about its strengths and weaknesses as they appear to the authors of this review.

Strengths

1. Obtains blade loads by finding basic isolated blade loads plus smaller linear perturbation loads due to tower motions.
2. Works with complete loads on blades from all sources, (aerodynamic, inertial, centrifugal, gravity, etc.)
3. Can include stall, variable inflow, and other aerodynamic nonlinearities.

4. Modular arrangement of components. Can handle all kinds of subpieces.
5. Good coupling and assembly of systems together. Uses good data processing methods. Numerical integration methods seem reasonable.
6. Includes frequency response methods for harmonic loads as well as time integration methods for load time histories.
7. Good procedure for obtaining correct initial conditions for steady-state solution.
8. Includes effects of periodic coefficients for forced response and possibly for stability investigations.

Weaknesses

1. Seems a reasonable, but somewhat cumbersome program. Very long, does everything numerically, most structural nonlinearities retained,* numerical differentiation may lead to small differences of large numbers, difficult to see what is causing what.
2. Many small couplings and effects are included which are probably unnecessary, but numerically complicating. Because allowance is made for so many features,

*Wind turbine blades are generally stiffer than helicopter blades. Can neglect many of the nonlinearities retained here by order of magnitude assumptions.

the program does things very generally and requires much data processing and sophisticated techniques to get answers.

3. Method is essentially a modal analysis for the blades. Use of at least 4 blade modes may be required for finding bending moments and shears on blades. This may tax the numerical capability of this program.
4. Quiescent position not consistently found in the analysis. Must get from elsewhere. Seems one is using very sophisticated additions to a crude model.
5. Need separate programs to obtain modes and quiescent position for the analysis. It seems the code should be able to get these for you, somewhere.
6. Teetering system seems inefficient in the operation of the system. Could perhaps be improved.
7. Some problems exist with the use of multiblade coordinates for 2-bladed rotors. The special form used in the program may be changed as discussed.
8. Possibility of flutter instability when there is a low torsional flexibility of the blade due to a loose pitch-change mechanism. Should be investigated more. Some question whether the system can model blade aeroelastic instabilities properly, since unsteady aerodynamic forces and wake interference effects may have to be included.

5. Recommendations

This report has attempted to give a review of the MOSTAS computer code for wind turbines, and to describe some of the techniques and methods used in its analyses. Also, some general methods used in wind turbine stability and response analyses have been reviewed. Based on this study, the following recommendations are suggested.

1. Make smaller, simpler models involving specific subcomponents, to investigate the main origin of large loads and instabilities. Try to understand what causes what by these simpler models.
2. Check out MOSTAS versus some simpler models to see what can be eliminated and simplified.
3. Look more into effects of aeroelastic flutter instabilities and also mechanical instabilities on these systems, especially with proposed soft, flexible mountings.
4. Look more closely at teetering effects and propeller whirl type flutter of these systems. This involves aeroelastic coupling with the tower yaw and pitch mechanisms.
5. Change the special form of the 2-bladed multiblade coordinate transformation used in the analysis, or use Floquet methods (or their equivalent) to analyze the stability of the response.

6. Improve teetering set-up if possible.
7. Look at drive train and torsional shaft-generator coupling problems more closely. These can probably be uncoupled from much of the tower motion dynamics.
8. Should calculate the quiescent position w_o by the computer code, for the given geometrical blade shape.

Appendix A

Stability and Response of Constant Coefficient Systems

Given a system of N linear differential equations with constant coefficients,

$$\underline{M}\ddot{\underline{q}} + \underline{B}\dot{\underline{q}} + \underline{K}\underline{q} = \underline{F}(t) \qquad \text{(A-1)}$$

where $\underline{M}$, $\underline{B}$, and $\underline{K}$ are the square matrices of order NxN, while $\underline{q}$ and $\underline{F}(t)$ are column matrices of order Nx1. These can be re-arranged as,

$$\begin{bmatrix} \underline{1} & 0 \\ 0 & \underline{M} \end{bmatrix} \begin{Bmatrix} \dot{\underline{q}} \\ \ddot{\underline{q}} \end{Bmatrix} - \begin{bmatrix} 0 & \underline{1} \\ -\underline{K} & -\underline{B} \end{bmatrix} \begin{Bmatrix} \underline{q} \\ \dot{\underline{q}} \end{Bmatrix} = \begin{Bmatrix} 0 \\ \underline{F} \end{Bmatrix} \qquad \text{(A-2)}$$

Then, multiplying through by the inverse of the mass matrix gives 2N first order equations,

$$\dot{\underline{y}} - \underline{A}\underline{y} = \underline{G} \qquad \text{(A-3)}$$

where $\underline{A}$ is a square matrix of order 2Nx2N, while $\underline{y}$ and $\underline{G}$ are column matrices of order 2Nx1 given by

$$\underline{A} = \begin{bmatrix} 0 & \underline{1} \\ -\underline{M}^{-1}\underline{K} & -\underline{M}^{-1}\underline{B} \end{bmatrix}, \quad \underline{y} = \begin{Bmatrix} \underline{q} \\ \dot{\underline{q}} \end{Bmatrix}, \quad \underline{G} = \begin{Bmatrix} 0 \\ \underline{M}^{-1}\underline{F} \end{Bmatrix} \qquad \text{(A-4)}$$

The above rearrangement, Eq.(A-3), is valid providing the mass $\underline{M}$ is not singular, which is usually the case with physical systems.

(a) Stability

To investigate stability, one sets $\underline{F} = 0$ (which gives

$\underline{G} = 0$) in Eq.(A-3) to obtain a set of homogeneous equations. Then one seeks exponential solutions of the form $\underline{y} = \underline{y}\, e^{pt}$. Placing these into Eq.(A-3) leads to the standard eigenvalue problem,

$$\underline{A}\,\underline{y} = p\,\underline{y} \tag{A-5}$$

Eigenvalues p_k of the matrix $\underline{A}$ can be obtained by standard numerical eigenvalue routines. If any eigenvalue p_k is positive real or has a positive real part, the system represented by Eq.(A-3) or equivalently by Eq.(A-1) is unstable.

(b) Forced Response

Under steady-state conditions, the forces $\underline{F}(t)$ on a rotating system tend to occur periodically in multiples of the rotation frequency Ω. One can then express the force for a particular frequency $\omega_m = m\Omega$, in the form,

$$\underline{F}(t) = \mathrm{Re}\left(\underline{F}\, e^{i\omega_m t}\right) = \underline{F}_R \cos\omega_m t - \underline{F}_I \sin\omega_m t \tag{A-6}$$

The response $\underline{q}(t)$ is similarly of the form,

$$\underline{q}(t) = \mathrm{Re}\left(\underline{q}\, e^{i\omega_m t}\right) = \underline{q}_R \cos\omega_m t - \underline{q}_I \sin\omega_m t \tag{A-7}$$

Placing Eqs.(A-6) and (A-7) into the basic Eq.(A-1) and matching sine and cosine terms gives a set of 2Nx2N real equations,

$$\begin{bmatrix} \underline{G} & \underline{H} \\ -\underline{H} & \underline{G} \end{bmatrix} \begin{Bmatrix} \underline{q}_R \\ \underline{q}_I \end{Bmatrix} = \begin{Bmatrix} \underline{F}_R \\ \underline{F}_I \end{Bmatrix} \tag{A-8}$$

where one has the matrix elements,

$$\underline{G} = \underline{K} - \omega_m^2 \underline{M} \quad , \quad \underline{H} = \omega_m \underline{B} \tag{A-9}$$

Given the amount of the m^{th} harmonic force present $\underline{F}_R^{(m)}$ and $\underline{F}_I^{(m)}$, Eq.(A-8) can be solved by simple inversion to find the response $\underline{q}_R^{(m)}$ and $\underline{q}_I^{(m)}$ for each harmonic. Then, one may sum up all the harmonics to give the total periodic response as,

$$\underline{q}(t) = \sum_{m=0}^{N} \underline{q}_R^{(m)} \cos \omega_m t - \sum_{m=0}^{N} \underline{q}_I^{(m)} \sin \omega_m t \tag{A-10}$$

Finding the response $\underline{q}(t)$ this way rather than by direct numerical integration, allows one to assess the effects of a particular harmonic on the resulting response of the system.

Appendix B

Floquet Methods for Periodic Coefficient Systems

Assume the coefficients $\underline{M}$, $\underline{B}$, $\underline{K}$ in Eq.(A-1) or equivalently the coefficients $\underline{A}$ in Eq.(A-3) vary periodically in time, rather than being constants. For illustrating Floquet methods, it will be convenient to use the first order representation, namely 2N equations of the form,

$$\dot{y} - \underline{A}(t)\, y = \underline{G}(t) \qquad \text{(B-1)}$$

where $\underline{A}(t)$ and $\underline{G}(t)$ are periodic over an interval T.

(a) Stability

The Floquet stability analysis described here follows that given by Peters and Hohenemser[12]. To investigate stability, one sets $\underline{G}=0$ in Eq.(B-1) to obtain homogeneous equations. The Floquet theorem states the solution of Eq.(B-1) with $\underline{G}=0$ is of the form

$$y(t) = \underline{B}(t)\left\{C_k\, e^{p_k t}\right\} \qquad \text{(B-2)}$$

where $\underline{y}(t)$ and $\{C_k e^{p_k t}\}$ are 2Nx1 column matrices, and $\underline{B}(t)$ is a 2Nx2N square matrix periodic over period T, that is, $\underline{B}(T)=\underline{B}(0)$. From the above, one can express

$$y(0) = \underline{B}(0)\left\{C_k\right\} \qquad \text{(B-3)}$$

$$y(T) = \underline{B}(T)\left\{C_k e^{p_k T}\right\} = \underline{B}(0)\left\{C_k e^{p_k T}\right\} \qquad \text{(B-4)}$$

Also, one can express $\underline{y}(T)$ as,

$$\underline{y}(T) = \underbrace{\left[\underline{y}^{(1)}\ \underline{y}^{(2)}\cdots\right]}_{[Q]} \begin{Bmatrix} y_1(0) \\ y_2(0) \\ \vdots \\ \vdots \end{Bmatrix} \tag{B-5}$$

where $\underline{y}^{(1)}$ is the solution at t=T of Eq.(B-1) with $\underline{G}$=0, for the initial conditions y_1=1 and all remaining $y_i(0)$=0, $\underline{y}^{(2)}$ is the solution for $y_2(0)$=1 and all remaining $y_i(0)$=0, etc. The square matrix [Q] is called the "Transition Matrix." Equating Eq.(B-5) to (B-4) and introducing Eq.(B-3) gives,

$$\begin{aligned}[Q]\left[\left\{B(0)\right\}_1 C_1 + \left\{B(0)\right\}_2 C_2 + \cdots\right] = \\ = \left\{B(0)\right\}_1 C_1 e^{P_1 T} + \left\{B(0)\right\}_2 C_2 e^{P_2 T} + \cdots\end{aligned} \tag{B-6}$$

Since C_k are independent, one must have

$$[Q]\left\{B(0)\right\}_{k} = \lambda_k \left\{B(0)\right\}_k \tag{B-7}$$

where $\lambda_k = e^{P_k T}$ are the eigenvalues of the [Q] matrix. One then has the relation

$$P_k = \frac{1}{T} \ln \lambda_k = \alpha_k + i\,\omega_k \tag{B-8}$$

from which the real and imaginary parts of the stability exponent P_k are given as

$$\alpha_k = \frac{1}{T} \ln|\lambda_k| = \frac{1}{2T} \ln\left[(\lambda_k)_R^2 + (\lambda_k)_I^2\right] \tag{B-9}$$

$$\omega_k = \frac{1}{T} \tan^{-1}\left[(\lambda_k)_I / (\lambda_k)_R\right] \qquad \text{(B-10)}$$

The real part α_k is a measure of the growth or decay of the response, as can be seen from Eq.(B-2). Values of $\alpha_k > 0$ (or equivalently $|\lambda_k| > 1$) indicate instability. The imaginary part ω_k represents the frequency. However, because $\tan^{-1}$ is multi-valued, one can only obtain ω_k to within a multiple of 2π. To obtain the actual frequency and motion corresponding to the k^{th} root, p_k, one sets $C_k=1$ and all other remaining $C_i=0$ in Eqs. B-2) and (B-3). Then, using the k^{th} eigenvector $\{B(0)\}_k$ from Eq.(B-7) as an initial condition, one would solve Eq.(B-1) with $\underline{G}=0$ by numerical integration techniques for the resultant motion.

Summarizing: To check for stability of a system of linear equations with periodic coefficients, obtain the eigenvalues λ_k of the "Transition Matrix" [Q]. If $|\lambda_k|>1$, one has instability. The traditional stability exponent p_k is related to λ_k through Eqs.(B-8) to (B-10). Two remarks on the above procedure should be noted. (1) The "Transition Matrix" [Q] can be formed by solving either the first order equations, Eqs.(B-1) with $\underline{G}=0$, or the second order equations, Eqs.(A-1) with $\underline{F}=0$ and periodic coefficients, whichever is more convenient for the integration scheme. (2) The above procedure will still apply even if the equations have constant coefficients. However, for such cases it is usually easier to form the matrix $\underline{A}$ given by Eq.(A-4) and obtain its eigenvalues p_k rather than to form the "Transition Matrix" [Q] and obtain its eigenvalues λ_k.

(b) Forced Response

Solutions of Eq.(B-1), or equivalently Eq.(A-1) with periodic coefficients, can be obtained by direct numerical integration using some convenient integration scheme. By proper choice of the initial conditions, one can eliminate all transients from the response and obtain the desired steady-state dynamic response by integrating through only one period T, instead of the very large number usually required to reach steady-state for lightly damped systems. A procedure for finding the proper initial conditions is given below.

Solutions of Eq.(B-1) are of the general form,

$$\underline{y}(t) = \underline{y}_H(t) + \underline{y}_P(t) \qquad \text{(B-11)}$$

where $\underline{y}_H(t)$ is the homogeneous solution and $\underline{y}_p(t)$ is the particular solution. One can obtain a complete solution of Eq.(B-1) numerically for any given set of initial conditions. Call this solution $\underline{y}_E(t)$. One can add any number of additional homogeneous solutions $\Delta\underline{y}_H(t)$ having different initial conditions, to this solution. This would give a new solution to Eq.(B-1),

$$\underline{y}(t) = \underline{y}_E(t) + \Delta\underline{y}_H(t) \qquad \text{(B-12)}$$

which would have different initial conditions than those of $\underline{y}_E(t)$.

One can obtain all the homogeneous solutions of Eq.(B-1) by solving Eq.(B-1) with $\underline{G}=0$ a total of 2N times, subject to the initial conditions $y_1=1$ and all remaining $y_i=0$, then $y_2=1$ and all remaining $y_i=0$, etc. In fact, this was done earlier

to investigate stability and resulted in the 2N homogeneous solutions $\underline{y}^{(1)}(t)$, $\underline{y}^{(2)}(t)$, etc., respectively. Thus, one may write

$$\Delta \underline{y}_H(t) = \underbrace{\left[\underline{y}^{(1)}(t) \quad \underline{y}^{(2)}(t) \cdots \right]}_{[Q(t)]} \begin{Bmatrix} C_1 \\ C_2 \\ \vdots \\ \vdots \end{Bmatrix} \tag{B-13}$$

where $[Q(t)]$ is the transition matrix at any instant of time, and C_1, C_2, ... are 2N arbitrary constants. The new solution Eq.(B-12) can be rewritten as

$$\underline{y}(t) = \underline{y}_E(t) + [Q(t)]\,\underline{C} \tag{B-14}$$

For a periodic solution over period $T=2\pi/\Omega$, one must have $\underline{y}(T)=\underline{y}(0)$. Placing Eq.(B-14) into this condition and solving for the arbitrary constants $\underline{C}$ gives,

$$\underline{y}_E(T) + [Q(T)]\,\underline{C} = \underline{y}_E(0) + [Q(0)]\,\underline{C} \tag{B-15}$$

$$\underline{C} = \left[\underline{1} - [Q] \right]^{-1} \left\{ \underline{y}_E(T) - \underline{y}_E(0) \right\}$$

where it was noted that $[Q(0)]=\underline{1}$, and $[Q(T)]=[Q]$ is the "Transition Matrix" found earlier for the stability investigation. Placing these values of $\underline{C}$ back into Eq.(B-14), the initial conditions for insuring a periodic solution become

$$\underline{y}(0) = \underline{y}_E(0) + \left[\underline{1} - \underline{Q} \right]^{-1} \left\{ \underline{y}_E(T) - \underline{y}_E(0) \right\} \tag{B-16}$$

One can then solve the basic Eq.(B-1) numerically with these initial conditions to obtain a periodic solution over one period. It should be noted that if one had chosen the initial conditions for $\underline{y}_E(t)$ as $\underline{y}_E(0)=0$, one would obtain simply,

$$\underline{y}(0) = \left[\underline{1} - \underline{Q}\right]^{-1} \underline{y}_E(T) \qquad \text{(B-17)}$$

This is particularly convenient form for finding the initial conditions for periodic solutions.

An alternative form for determining the proper initial conditions for periodic solutions has been proposed by Friedmann and his coworkers[5,6] in their work on wind turbines, namely,

$$\underline{y}(0) = \left[\underline{1} - \underline{Q}\right]^{-1} \underline{Q} \int_0^T \left[Q(t)\right]^{-1} \underline{F}(t)\, dt \qquad \text{(B-18)}$$

This is similar to Eq.(B-17), but does not use $\underline{y}_E$. It seems easier to obtain $\underline{y}_E(T)$ with initial conditions $\underline{y}_E(0)=0$ and use Eq.(B-17), rather than obtaining [Q(t)] at every point and performing the indicated operations required by Eq.(B-18).*

The general procedure described by Eqs.(B-11) to (B-17) may be extended to deal also with nonlinear equations,

$$\dot{\underline{y}} - \underline{A}(t)\,\underline{y} = \underline{F}(t, \underline{y}, \dot{\underline{y}}) \qquad \text{(B-19)}$$

where the right hand side now contains nonlinear functions of the coordinates. An iterative variation of the previous linear procedure to obtain the initial conditions for periodic solutions

---

*A comparison of these methods as well as a similar general derivation was given by Izadpanah (Ref. 13). This was pointed out to the authors by Prof. D. A. Peters of Washington University, Saint Louis, Missouri.

of nonlinear equations is used by the MOSTAS Code[1]. The procedure is as follows. First, a numerical solution $\underline{y}_E(t)$ is obtained to the nonlinear Eq.(B-19) for some estimate of the initial conditions $\underline{y}_E(0)$. Then each of the 2N elements of $\underline{y}_E(0)$ is perturbed a small amount ϵ_i and the resulting 2N solutions are obtained. This involves solving the nonlinear Eq.(B-19) subject to the initial conditions,

$$\underline{y}_E(0) + \begin{Bmatrix} \epsilon_1 \\ 0 \\ 0 \\ \vdots \end{Bmatrix}, \quad \underline{y}_E(0) + \begin{Bmatrix} 0 \\ \epsilon_1 \\ 0 \\ \vdots \end{Bmatrix}, \text{ etc.} \tag{B-20}$$

and will result in 2N responses of the form

$$\underline{y}^{(i)}(t) = \underline{y}_E(t) + \Delta \underline{y}_E^{(i)}(t) \tag{B-21}$$

where $\Delta \underline{y}_E^{(i)}(t)$ represents the effect of each perturbation ϵ_i, and is found by subtracting $\underline{y}_E(t)$ from each of the 2N resulting responses $\underline{y}^{(i)}(t)$. One can then express the total solution approximately as,

$$\underline{y}(t) = \underline{y}_E(t) + \underbrace{\left[\frac{1}{\epsilon_1}\Delta \underline{y}_E^{(1)}, \frac{1}{\epsilon_2}\Delta \underline{y}_E^{(2)}, \cdots\right]}_{[Q]} \begin{Bmatrix} \epsilon_1 \\ \epsilon_2 \\ \vdots \end{Bmatrix} \tag{B-22}$$

which is in the same form as Eq.(B-13). Then, again requiring the periodicity condition $\underline{y}(T)=\underline{y}(0)$ and following through as before, will result in the same relation Eq.(B-16) found

previously. Because of the nonlinearities now present, the elements of [Q] as found from Eqs.(B-22), (B-21), (B-20) may vary with the amplitude of the initial condition used, $\underline{y}_E(0)+\underline{\varepsilon}_i$. This is in contrast to the linear case where [Q] remains always constant. Hence, an iterative application of Eq.(B-16) with a new corrected $\underline{q}_E(0)$ should be done. If the nonlinearities are not too great, convergence to the required $\underline{y}_E(0)$ should be rapid.

It should be remarked that the numerical procedure for forced response described in this section can also be used for the constant coefficient linear case, although it is probably easier there to obtain the solution by using Harmonic response methods given by Eqs. (A-6) to (A-10). However, for cases where there is some nonlinearity, the present iterative approach becomes attractive.

Summarizing, the Floquet methods described in this Appendix are based on a convenient numerical integration scheme and involve the computation of the "Transition Matrix," [Q], from which both stability and the initial conditions for steady-state response solutions can be obtained. These methods seem attractive for large systems and can be modified to include nonlinearities in the equations.

Appendix C

Multiblade Coordinates and Harmonic Balance Methods

Given a rotor with N blades rotating with rotation speed Ω, attached to a flexible tower. Because the tower motions x_i are described in a fixed reference frame while the blade motions β_i are described relative to a rotating frame, the resulting equations may have mass, damping, or stiffness coefficients which are functions of the azimuthal position of the k^{th} blade ψ_k. A typical such set of equations is given, for example, in Refs. 4 and 14 as,

$$M\ddot{x} + C_x\dot{x} + k_x x + S\frac{d^2}{dt^2}\sum^{k} \beta^{(k)} \cos\psi_k = F_x(t)$$

$$S\ddot{x}\cos\psi_k + I\ddot{\beta}^{(k)} + C_\beta\dot{\beta}^{(k)} + k_\beta\beta^{(k)} = F_\beta^{(k)}(t) \qquad (C\text{-}1)$$

$$(k = 1, 2, \cdots N)$$

where the azimuthal position ψ_k is,

$$\psi_k = \Omega t + (k-1)2\pi/N \qquad (C\text{-}2)$$

The first equation above represents force equilibrium for the tower motion x, while the remaining N equations represent force equilibrium for the motion of each of the N blades $\beta^{(k)}$. The above equations are readily generalized to more tower motions x_i, and more blade coordinates for each blade $\beta_i^{(k)}$.

(a) Stability

To examine Eqs.(C-1) for stability, one sets $F_x=0$ and $F_\beta^{(k)}=0$ to obtain homogeneous equations.

For rotors with 3 or more blades $N\geq 3$, one may eliminate the periodic coefficients in these equations by introducing new multiblade coordinates $b_T(t)$, $b_{1s}(t)$, $b_{1c}(t)$, $b_{2s}(t)$, ... such that

$$\beta^{(k)} = b_T(t) + b_{1s}(t)\sin\psi_k + b_{1c}(t)\cos\psi_k + b_{2s}(t)\sin 2\psi_k + b_{2c}(t)\cos 2\psi_k + \cdots + b_A(-1)^{k-1} \tag{C-3}$$

where the total number of coordinates b_i taken is equal to the number of blades, N. Note, if N = even number, then the additional mode $(-1)^{k-1}b_A$ is needed to complete the set. The above form is an equivalent modal representation of the N blades. Substituting these into Eqs.(C-1), then multiplying the last N equations by $\sin\psi_k$, $\cos\psi_k$, 1, $\sin 2\psi_k$, $\cos 2\psi_k$, ... $(-1)^{k-1}$ respectively, then summing these last N equations and noting the trigonometric identities,

$$\begin{aligned}
\sin m\psi_k \sin n\psi_k &= \tfrac{1}{2}\cos(m-n)\psi_k - \tfrac{1}{2}\cos(m+n)\psi_k \\
\sin m\psi_k \cos n\psi_k &= \tfrac{1}{2}\sin(m-n)\psi_k + \tfrac{1}{2}\sin(m+n)\psi_k \\
\cos m\psi_k \sin n\psi_k &= -\tfrac{1}{2}\sin(m-n)\psi_k + \tfrac{1}{2}\sin(m+n)\psi_k \\
\cos m\psi_k \cos n\psi_k &= \tfrac{1}{2}\cos(m-n)\psi_k + \tfrac{1}{2}\cos(m+n)\psi_k
\end{aligned} \tag{C-4}$$

$$
\begin{aligned}
\sum_{k=1}^{N} \sin m\psi_k &= \begin{cases} N \sin m\psi_1 & \text{for } m = N, 2N, \cdots \\ 0 & \text{for } m \neq N, 2N, \cdots \end{cases} \\
\sum_{k=1}^{N} \cos m\psi_k &= \begin{cases} N \cos m\psi_1 & \text{for } m = N, 2N, \cdots \\ 0 & \text{for } m \neq N, 2N, \cdots \end{cases} \\
\sum_{k=1}^{N} (-1)^{k-1} \sin m\psi_k &= \begin{cases} N \sin m\psi_1 & \text{for } m = N/2, 3N/2, \cdots \\ 0 & \text{for } m \neq N/2, 3N/2, \cdots \end{cases} \\
\sum_{k=1}^{N} (-1)^{k-1} \cos m\psi_k &= \begin{cases} N \cos m\psi_1 & \text{for } m = N/2, 3N/2, \cdots \\ 0 & \text{for } m \neq N/2, 3N/2, \cdots \end{cases}
\end{aligned}
\qquad \text{(C-4)}
$$

results in a new set of differential equations in the variables x, b_{1s}, b_{1c}, b_T, b_{2s}, b_{2c} $\cdots$ b_A, which for $N \geq 3$ blades, now all have constant coefficients namely,

$$
\begin{aligned}
& M\ddot{x} + C_x \dot{x} + k_x x + \frac{N}{2} S \ddot{b}_{1c} = 0 \\
& \frac{N}{2}\left[I\ddot{b}_{1s} + C_\beta \dot{b}_{1s} + (k_\beta - I\Omega^2)\beta_{1s} - 2\Omega I \dot{b}_{1c} - \Omega C_\beta b_{1c} \right] = 0 \\
& \frac{N}{2}\left[S\ddot{x} + 2\Omega I \dot{b}_{1s} + \Omega C_\beta b_{1s} + I\ddot{b}_{1c} + C_\beta \dot{b}_{1c} + (k_\beta - I\Omega^2) b_{1c} \right] = 0 \\
& N\left[I\ddot{b}_T + C_\beta \dot{b}_T + k_\beta b_T \right] = 0 \\
& \frac{N}{2}\left[I\ddot{b}_{2s} + C_\beta \dot{b}_{2s} + (k_\beta - 4I\Omega^2) b_{2s} - 4\Omega I \dot{b}_{2c} - 2\Omega C_\beta b_{2c} \right] = 0 \\
& \qquad \vdots \\
& N\left[I\ddot{b}_A + C_\beta \dot{b}_A + k_\beta b_A \right] = 0
\end{aligned}
\qquad \text{(C-5)}
$$

These equations may then be investigated for stability using the standard constant coefficient techniques described earlier. It should be noted that because of the form of Eqs.(C-1), the equations above uncouple into several smaller groups, and in fact only the first three equations above are coupled together and involve the tower motion variable x. For additional details and applications of multiblade coordinates, see Hohenemser and Yin[3] and Johnson[15]. Multiblade coordinates were originally introduced by Coleman and Feingold[16] in their studies of helicopter ground resonance.

For rotors with 2 blades, N=2, the analysis is more difficult because the rotor disk no longer has polar symmetry. For this case, one may use multiblade coordinates together with harmonic balance methods to arrive at approximate solutions. The multiblade transformation Eq.(C-3) for 2 blades can be expressed in terms of coordinates $b_T(t)$ and $b_A(t)$ as,

$$\beta^{(1)} = b_T + b_A \quad , \qquad \beta^{(2)} = b_T - b_A \tag{C-6}$$

These coordinates are introduced into Eqs.(C-1), then summing and subtracting the last two equations of Eqs.(C-1) respectively while noting that $\sin \psi_2 = -\sin \psi_1$ and $\cos \psi_2 = -\cos \psi_1$ results in a new set of differential equations in the variables x, b_T, b_A which still have periodic coefficients. Then, expanding each of the coordinates in a harmonic series,

$$\chi = \chi_o + \chi_{1S} \sin\Omega t + \chi_{1C} \cos\Omega t + \chi_{2S} \sin 2\Omega t + \cdots$$

$$b_T = b_{TO} + b_{T1S} \sin\Omega t + b_{T1C} \cos\Omega t + b_{T2S} \sin 2\Omega t + \cdots \quad \text{(C-7)}$$

$$b_A = b_{AO} + b_{A1S} \sin\Omega t + b_{A1C} \cos\Omega t + b_{A2S} \sin 2\Omega t + \cdots$$

where x_o, x_{1s}, b_{TO}, b_{T1S}, ... are all functions of time, then placing these into the previous equations and balancing out each harmonic term in each equation, will yield an infinite set of constant coefficient differential equations which can be truncated at some point for approximate solutions. These truncated equations may again be examined for stability using the standard constant coefficient techniques described earlier.

Often, depending on the form of Eqs.(C-1), the resulting constant coefficient differential equations will uncouple into several smaller coupled systems of equations which may be examined independently of one another. For example, for the case of Eqs.(C-1), one smaller coupled system would involve the variables x_0, x_{2S}, x_{2C}, b_{A1S}, b_{A1C}, ... while another would involve x_{1C}, x_{1S}, b_{AO}, b_{A2S}, b_{A2C}, ... For such systems, one could use an alternate extended form of the multiblade coordinate transformation Eq.(C-3) namely,

$$\chi = \chi_o + \chi_{2S} \sin 2\Omega t + \chi_{2C} \cos 2\Omega t + \cdots$$

$$\beta^{(k)} = b_{1S} \sin\psi_k + b_{1C} \cos\psi_k + b_{3S} \sin 3\psi_k + \cdots \quad \text{(C-8)}$$

together with the harmonic balance method to solve the problem. This works here, since the form given by Eq.(C-8) exactly duplicates the motion of the two blades given by the general case Eqs.(C-6) and (C-7), since sin ψ_2 = -sin ψ_1, cos ψ_2 = -cos ψ_1, and only x_o, x_{2S}, x_{2C}, b_{AlS}, b_{AlC}, ... would be present. See Sheu[4] for an application of this alternate extended form of the multiblade transformation Eq.(C-8) to a simple two-bladed rotor in ground resonance, Eqs.(C-1). Solutions involving as little as three terms, x_o, b_{ls}, b_{lc}, gave reasonable approximations to the primary instability regions. However, in more general cases (for example, if the first equation of Eqs.(C-1) had an additional terms $M_1\ddot{x}$ cos ψ_1 or k_1x cos ψ_1 present), the resulting equations would not split into two smaller groups, and the general harmonic balance method Eqs.(C-6) and (C-7) would have to be used.

Indeed, for the more general case mentioned above, one would also investigate the system for direct Mathieu equation type instabilities of half integer order $\Omega/2$, $3\Omega/2$, ... by introducing additional harmonic terms sin $m\Omega t$ and cos $m\Omega t$ where m=1/2, 3/2, 5/2, ... into Eqs.(C-7), and harmonically balancing as before. These terms would not couple in with the previous equations and can be solved independently of them. The primary instability region would result from the $\Omega/2$ terms. See Bolotin[17] for further details of the general harmonic balance method.

$$
\begin{aligned}
x &= x_R \cos\omega_m t - x_I \sin\omega_m t \\
\beta^{(k)} &= b_{TR}\cos\omega_m t - b_{TI}\sin\omega_m t \\
&\quad + \left(b_{1sR}\cos\omega_m t - b_{1sI}\sin\omega_m t\right)\sin\psi_k \\
&\quad + \left(b_{1cR}\cos\omega_m t - b_{1cI}\sin\omega_m t\right)\cos\psi_k \\
&\quad + \left(b_{2sR}\cos\omega_m t - b_{2sI}\sin\omega_m t\right)\sin 2\psi_k + \cdots
\end{aligned}
\qquad \text{(C-11)}
$$

The tower thus oscillates at frequency ω_m in the fixed frame whereas the blades may oscillate at frequencies ω_m, $\omega_m + \Omega$, $\omega_m - \Omega$, $\omega_m + 2\Omega$, $\omega_m - 2\Omega$, ... relative to the rotating frame, depending on which coordinates b_i are excited. For example, in the case of a 3 bladed rotor N=3, the $F_{\beta 1C}$ term of Eq.(C-10) leads to a constant term on the right-hand-side which excites the x, b_{1s}, b_{1c} coordinates and results in a constant x and a $\beta^{(k)}$ frequency of Ω, while the $F_{\beta 2C}$ term leads to a cos 3ψ term on the right-hand-side which again excites x, b_{1s}, b_{1c} and results in an x frequency of 3Ω and $\beta^{(k)}$ frequencies of 2Ω, 4Ω.

For rotors with 2 blades N=2, one can use the harmonic balance methods of the previous section. The steady-state periodic tower and blade forces given by Eqs.(C-10) are substituted into the basic equations of motions [Eqs.(C-1)]. One then introduces the new coordinates given by Eqs.(C-6), then sums and subtracts the last two blade equations, then expands the tower and blade motions as given by Eq.(C-7), only now the coordinates x_0, x_{1S}, b_{TO}, b_{T1S}, b_{AO}, ... etc. are taken

to be constants rather than functions of time. Harmonically balancing the various terms in each equation results in a truncated set of algebraic equations which can be solved to obtain the coordinates x_o, x_{1s}, b_{To}, ... etc., corresponding to the given forcing excitations F_{xo}, F_{x1s}, $F_{\beta o}$, $F_{\beta o}$, $F_{\beta 1s}$, ... etc. The resulting tower and blade motions are then given directly by Eqs.(C-7) and (C-6). The resulting set of algebraic equations will often uncouple into smaller coupled sets of equations which can be examined independently of one another. This procedure is similar to that for the constant coefficient forced response case Eq.(A-8), except now, the periodic coefficients couple the different harmonics together. Thus, the solution will consist of many harmonics $m\Omega$ even if only one forcing harmonic $F_{\beta 1s}$ were present alone.

Summarizing, the multiblade coordinate and harmonic balance methods described in this Appendix involve first the introduction of multiblade coordinates in order to take out the periodic coefficients from the blades [Eqs.(C-3) for $N \geq 3$], or to obtain a better ordered system of equations [Eqs.(C-6) for N=2]. Then harmonic balance methods Eqs.(C-7) are used to deal with any remaining periodic coefficients. These methods seem attractive for smaller systems and can give considerable insight into the origin and nature of instabilities and the various harmonics present in the forced response.

Appendix D

Rotating Coordinates

As an addendum to the previous multiblade coordinates and harmonic balance methods, it should be mentioned that for some problems, the use of rotating coordinates is also convenient. For example, in the case of a 2-bladed rotor on isotropic tower supports (same tower mass, damping, and stiffness in two directions, x_1 and x_2), Eqs.(C-1) would read,

$$
\begin{aligned}
&M\ddot{x}_1 + C_x\dot{x}_1 + k_x x_1 + S\frac{d^2}{dt^2}\sum^{k} \beta^{(k)} \cos\psi_k = F_{x1}(t) \\
&M\ddot{x}_2 + C_x\dot{x}_2 + k_x x_2 - S\frac{d^2}{dt^2}\sum^{k} \beta^{(k)} \sin\psi_k = F_{x2}(t) \qquad \text{(D-1)} \\
&S\ddot{x}_1 \cos\psi_k - S\ddot{x}_2 \sin\psi_k + I\ddot{\beta}^{(k)} + C_\beta\dot{\beta}^{(k)} + k_\beta\beta^{(k)} = F_\beta^{(k)}(t) \\
&\qquad\qquad (k = 1, 2, \cdots N)
\end{aligned}
$$

One can then express the tower motions x_1 and x_2 in terms of rotating coordinates ξ_1 and ξ_2 which rotate with the rotor, as

$$
\begin{aligned}
x_1 &= \xi_1 \cos\Omega t + \xi_2 \sin\Omega t \\
x_2 &= -\xi_1 \sin\Omega t + \xi_2 \cos\Omega t \qquad \text{(D-2)}
\end{aligned}
$$

where the rotation $\psi_1 = \Omega t$ is taken from the x_2 axis towards the x_1 axis. Placing these equations into Eqs.(D-1), then

multiplying the first two equations by cos ψ_1 and sin ψ_1 respectively and subtracting, then multiplying the first two equations by sin ψ_1 and cos ψ_1 and adding, then subtracting the third and fourth equations, then adding the third and fourth equations will result in a new set of differential equations in the variables ξ_1, ξ_2, b_A, b_T which now all have constant coefficients, namely,

$$M(\ddot{\xi}_1 + 2\Omega\dot{\xi}_2 - \Omega^2\xi_1) + C_x(\dot{\xi}_1 + \Omega\xi_2) + k_x\xi_1 + 2S(\ddot{b}_A - \Omega^2 b_A) = F_{x1}\cos\Omega t - F_{x2}\sin\Omega t$$

$$M(\ddot{\xi}_2 - 2\Omega\dot{\xi}_1 - \Omega^2\xi_2) + C_x(\dot{\xi}_2 - \Omega\xi_1) + k_x\xi_2 - 4S\Omega\dot{b}_A = F_{x1}\sin\Omega t + F_{x2}\cos\Omega t \qquad \text{(D-3)}$$

$$2S(\ddot{\xi}_1 + 2\Omega\dot{\xi}_2 - \Omega^2\xi_1) + 2I\ddot{b}_A + 2C_\beta\dot{b}_A + 2k_\beta b_A = F_\beta^{(1)} - F_\beta^{(2)}$$

$$2I\ddot{b}_T + 2C_\beta\dot{b}_T + 2k_\beta b_T = F_\beta^{(1)} + F_\beta^{(2)}$$

In the above, $b_T = [\beta^{(1)} + \beta^{(2)}]/2$ and $b_A = [\beta^{(1)} - \beta^{(2)}]/2$ are the same coordinates introduced earlier in Eqs.(C-6). These differential equations may then be investigated for stability

and forced response using the standard constant coefficient techniques described earlier. Such analyses of a 2-bladed rotor on isotropic tower supports were also performed by Coleman and Feingold[16] in their studies of helicopter ground resonance.

Rotating coordinates are often used in rotating machinery shaft critical speed problems, and are useful for dealing with problems of rotors with unsymmetrical mass, unsymmetrical damping, or unsymmetrical shaft stiffness supported on isotropic bearings. See for example, Bolotin[18]. For such problems, one can readily set up the equations of motion in the rotating frame directions, and the fixed supports will introduce no periodic terms because of their isotropic nature. For vertical axis wind turbines, such rotating coordinates for the blades are useful since the tower supports are generally isotropic due to the symmetrically arranged guy wires. For horizontal axis wind turbines, the tower supports are generally not isotropic, hence periodic coefficients will remain in the equations when using rotating coordinates. If the support anisotropy is not too large, one can again additionally introduce harmonic balance methods to eliminate the periodic coefficients, as was done in the previous section.

Summarizing, the rotating coordinates described in this Appendix can also be used to effectively eliminate the periodic coefficients in problems involving unsymmetrical rotors on isotropic tower supports. These can often be used in rotating

shaft critical speed problems and for vertical axis wind turbines. If the support anisotropy is not too large, harmonic balance methods may additionally be used to deal with any remaining periodic coefficients.

References

1 Hoffman, J.A., Dreier, M.E., Williamson, D.R., and Henninger, W.C., "Mathematical Methods Incorporated in the Wind Energy System Coupled Dynamics Analysis," Paragon Pacific Inc. Report PPI-1014-7, January 1977.

2 Kaza, K.R.V., Janetzke, D.C., and Sullivan, T.L., "Evaluation of MOSTAS Computer Code for Predicting Dynamic Loads in Two-Bladed Wind Turbines," DOE/NASA/1028-79/2, NASA TM-79101, April 1979. (Also, J. of Energy, Vol. 4, No. 4, July-August 1980, pp 162-169).

3 Hohenemser, K.H. and Yin, S.K., "Some Applications of the Method of Multiblade Coordinates," J. American Helicopter Society, July 1972, pp 3-12.

4 Sheu, D.L., "Wind Energy Conversion, Vol. 7: Effects of Tower Motion on the Response of Windmill Rotor," M.I.T. Aeroelastic and Structures Research Laboratory Report ASRL-TR-184-13. U.S. Department of Energy Report COO-4131-T1 (Vol. 7), September 1978.

5 Kottapalli, S.B.R., Friedmann, P.P., and Rosen, A., "Aercelastic Stability and Response of Horizontal Axis Wind Turbine Blades," AIAA J., Vol. 17, No. 12, December 1979, pp 1381-1389.

6 Warmbrodt, W. and Friedmann, P.P., "Coupled Rotor/Tower Aeroelastic Analysis of Large Horizontal Axis Wind Turbines," AIAA J., Vol. 18, No. 9, September 1980, pp 1118-1124.

7 Bielewa, R.L., "Blade Stress Calculations - Mode Deflection vs. Force Integration," J. American Helicopter Society, July 1978, pp 10-16.

8 Spera, D.A., "Structural Analysis of Wind Turbine Rotors for NSF-NASA Mod-O Wind Power System," DOE/NASA/1004-77/4, NASA TM X-3198, March 1975.

9 Miller, R.H. et al, "Wind Energy Conversion, Vol. 1: Methods for Design Analysis of Horizontal Wind Axis Turbines," MIT Aeroelastic and Structures Research Laboratory Report ASRL TR-184-7. U.S. Dept. of Energy Report COO-4131-T1, (Vol. 1), September 1978.

10 Friedmann, P.P., "Aeroelastic Stability and Response Analysis of Large Horizontal Axis Wind Turbines," J. of Industrial Aerodynamics, January 1980, pp 373-401.

11 Hoffman, J.A., "Linear Analysis Software System (LASS) Technical Documentation and User's Guide," Paragon Pacific Inc. Report PPI-1013-4, November 1975.

12 Peters, D.A. and Hohenemser, K.H., "Application of the Floquet Transition Matrix to Problems of Lifting Rotor Stability," J. American Helicopter Society, Vol. 16, No. 2, April 1971, pp 25-33.

13 Izadpanah, A.P., "Helicopter Trim and Air Loads by Periodic Shooting with Newton-Raphson Iteration," MS Thesis, Sever Institute of Technology, Washington University, St. Louis, Missouri, December 1979.

14 Miller, R.H., Dugundji, J., Chopra, I., Sheu, D.L. and Wendell, J.H., "Wind Energy Conversion, Vol. 3: Dynamics of Horizontal Axis Wind Turbines," MIT Aeroelastic and Structures Research Laboratory Report ASRL TR 184-9. U.S. Dept. of Energy Report COO-4131-T1 (Vol. 3), September 1978.

15 Johnson, W., Helicopter Theory, Princeton University Press, Princeton, NJ, 1980, Chaps. 8 and 12.

16 Coleman, R.P. and Feingold, A.N., "Theory of Self-Excited Mechanical Oscillations of Helicopter Rotors with Hinged Blades," NACA Technical Report TR 1351, 1958.

17 Bolotin, V.V., The Dynamic Stability of Elastic Systems, Holden-Day, Inc., San Francisco, 1964, Chaps. 1 and 14.

18 Bolotin, V.V., Nonconservative Problems of the Theory of Elastic Stability, MacMillan Co., New York, 1963, Chap. 3.

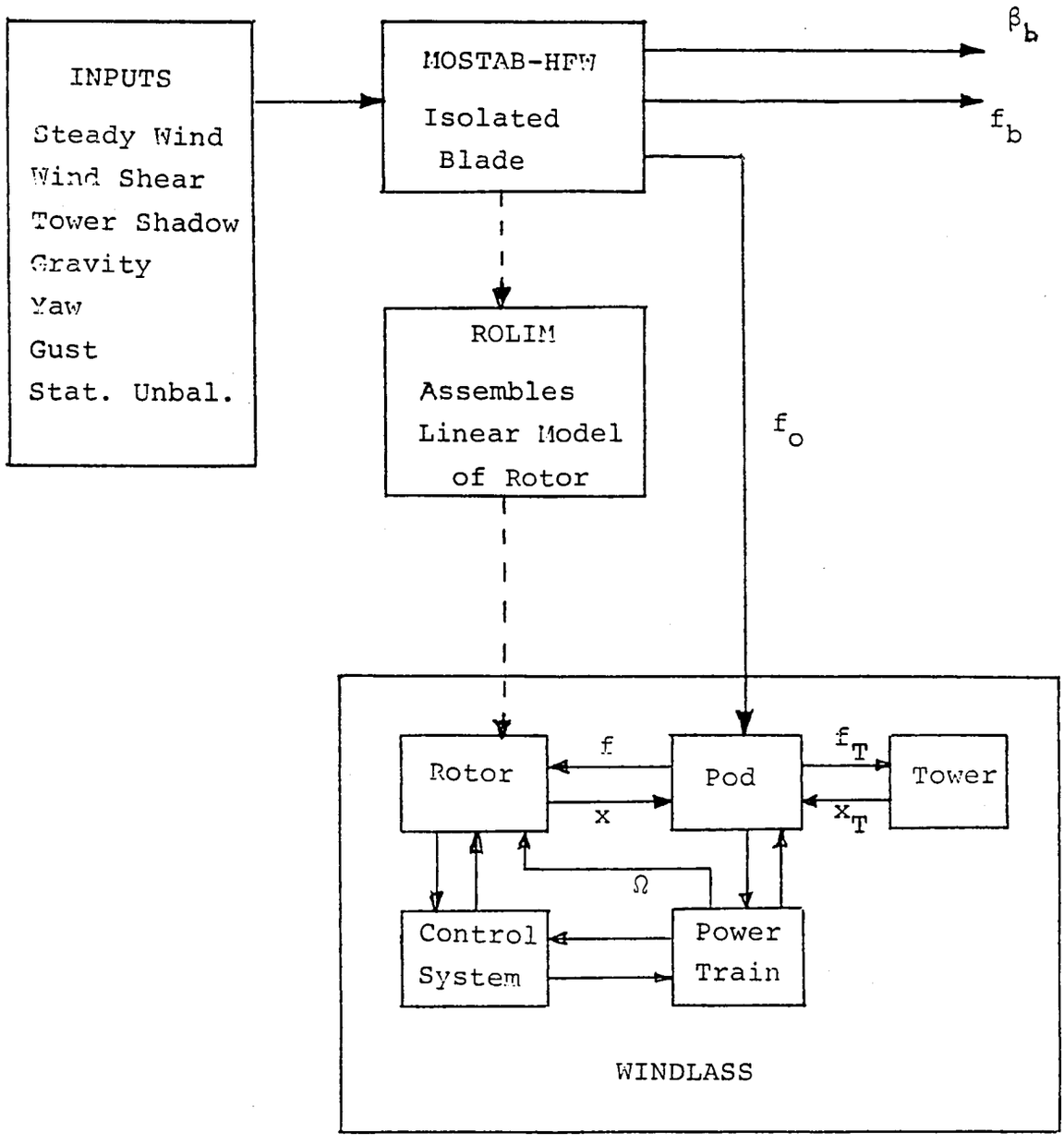

f_o -- Total rotor load at fixed shaft

f -- Perturbation pod load applied to rotor

f_b -- Fixed shaft blade load

$\tilde{f}$ -- Perturbation blade load

f_{TOT} -- $f_b + \tilde{f}$

β_b -- Fixed shaft blade coord.

x -- Rotor shaft displace.

Ω -- Rotation speed

FIG. 1 Layout of MOSTAS Computer Code

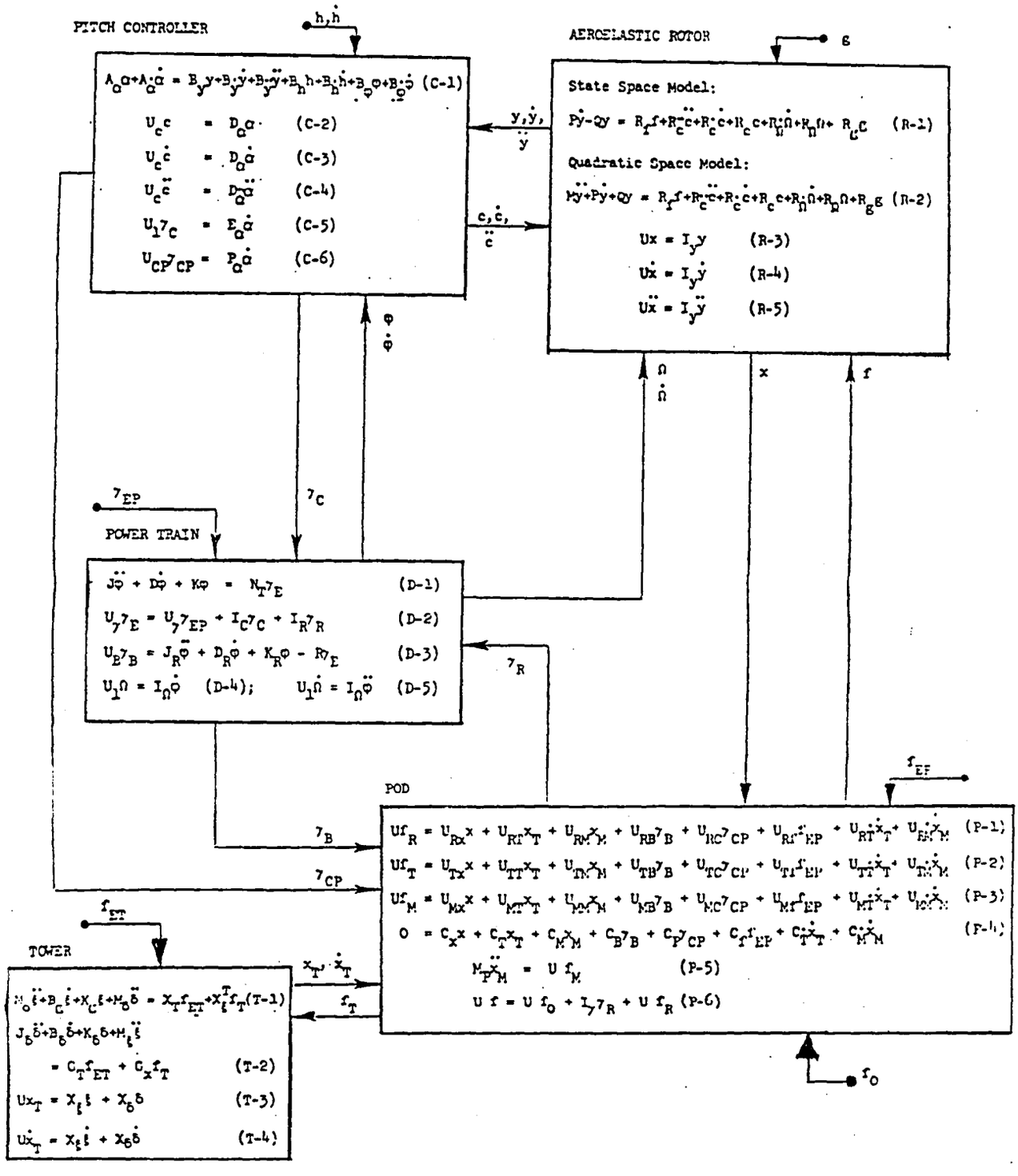

FIG. 2 WINDLASS System Block Diagram

1. Report No.	2. Government Accession No.	3. Recipient's Catalog No.
NASA CR-165385		

4. Title and Subtitle	5. Report Date
GENERAL REVIEW OF THE MOSTAS COMPUTER CODE FOR WIND TURBINES	June 1981
	6. Performing Organization Code

7. Author(s)	8. Performing Organization Report No.
John Dugundji and John H. Wendell	ASRL TR 197-1
	10. Work Unit No.

9. Performing Organization Name and Address	11. Contract or Grant No.
Aeroelastic and Structures Research Laboratory Department of Aeronautics and Astronautics Massachusetts Institute of Technology Cambridge, MA 02139	NSG-3303
	13. Type of Report and Period Covered
12. Sponsoring Agency Name and Address	Contractor Report
U.S. Department of Energy Division of Wind Energy Systems Washington, D.C. 20545	14. Sponsoring Agency Code Report No.
	DOE/NASA/3303-1

15. Supplementary Notes

Technical Memorandum. Prepared under Interagency Agreement DE-AI01-76ET20320. Project Manager, D. Janetzke, Wind Energy Project Office, NASA Lewis Research Center, Cleveland, Ohio 44135

16. Abstract

The MOSTAS computer code for wind turbine analysis is reviewed, and the techniques and methods used in its analyses are described in some detail. Some impressions of its strengths and weakness, & some recommendations for its application, modification, & further development are made. Additionally, some basic techniques used in wind turbine stability and response analyses for systems with constant and periodic coefficients are reviewed in the Appendices.

17. Key Words (Suggested by Author(s))	18. Distribution Statement
Wind Turbine Dynamic Loads Wind Turbine Aeroelasticity Structural Dynamics Aeroelasticity	Unclassified - unlimited STAR Category 44 DOE Category UC-60

19. Security Classif. (of this report)	20. Security Classif. (of this page)	21. No. of Pages	22. Price*
Unclassified	Unclassified	73	

* For sale by the National Technical Information Service, Springfield, Virginia 22161

End of Document